International Journal of Engineering Innovation & Research
Volume 5, Issue 1, ISSN: 2277 – 5668

# Failure of Local Sharp-cut 6061-T6 Aluminum Alloy Tubes Subjected to Cyclic Bending

**Kuo-Long Lee**
Professor, Dept. of Innovative Design and Entrepreneurship Management, Far East University, Tainan, Taiwan
Email:lkl@cc.feu.edu.tw

**Li-Yang Chen**
Grad. Student, Dept. of Engineering Science, National Cheng Kung University, Tainan, Taiwan
Email: mickey821994@gmail.com

**Wen-Fung Pan**
Professor, Dept. of Engineering Science National Cheng Kung University, Tainan, Taiwan
Email: z7808034@email.ncku.edu.tw

***Abstract*** **- In this paper, local sharp-cut 6061-T6 aluminum alloy tubes with different cut depths subjected to cyclic bending was experimentally and theoretically investigated. The tube-bending machine and curvature-ovalization measurement apparatus were used to conduct the curvature-controlled cyclic bending test. Five different cut depths of 0.4, 0.8, 1.2, 1.6 and 2.0 mm were considered. The finite element software ANSYS was used to analyze the moment-curvature and ovalization-curvature relationships. Because the failure type was the fatigue fracture, the ANSYS was used to calculate the maximum and minimum stresses for each cyclic bending case. Finally, a simple fatigue model was proposed for predicting the fatigue life of local sharp-cut 6061-T6 aluminum alloy tubes with different cut depths subjected to cyclic bending.**

***Keywords*** **– 6061-T6 Aluminum Alloy Tubes, Local Sharp-Cut, Cyclic Bending, Moment, Curvature, Finite Element ANSYS Analysis, Fatigue Model.**

## I. INTRODUCTION

In 1985, Shaw and Kyriakides [1] designed and constructed a tube cyclic bending machine and conducted a series of experimental and theoretical investigations. Kyriakides and Shaw [2] later investigated the inelastic behavior of tubes subjected to cyclic bending and extended the analysis of tubes to stability conditions under cyclic bending. Corona and Kyriakides [3] investigated the stability of tubes subjected to combined bending and external pressure; they also later [4] studied the degradation and buckling of tubes under cyclic bending and external pressure. Corona and Vaze [5] studied the response, buckling, and collapse of long, thin-walled seamless steel square tubes under bending. Later they [6] experimentally investigated the elastic-plastic degradation and collapse of steel tubes with square cross-sections under cyclic bending. Corona and Kyriakides [7] also studied the asymmetric collapse modes of pipes under combined bending and pressure. Corona *et al.* [8] conducted a set of bending experiments on aluminum alloy tubes to investigate the yield anisotropy effects on buckling. Later, Kyriakides *et al.* [9] studied the plastic bending of steel tubes with a diameter-to-thickness ratio ($D_o/t$ ratio) of 18.8, exhibiting Lüders bands through the experiment. Limam *et al.* [10] studied the inelastic bending and collapse of tubes in the presence of bending and internal pressure. Hallai *et al.* [11] experimentally studied the effect of Lüders bands on the bending of steel tubes. Limam *et al.* [12] later investigated the collapse of dented tubes under combined bending and internal pressure. Bechle and Kyriakides [13] later studied the localization of NiTi tubes subjected to bending.

In 1998, Pan *et al.* [14] designed and set up a new measurement apparatus. It was used with the cyclic bending machine to study various kinds of tubes under different cyclic bending conditions. For instance, Pan and Fan [15] studied the effect of the prior curvature-rate at the preloading stage on subsequent creep (moment is kept constant for a period of time) or relaxation (curvature is kept constant for a period of time) behavior, Pan and Her [16] investigated the response and stability of SUS304 stainless steel tubes that were subjected to cyclic bending with different curvature-rates, Lee *et al.* [17] studied the influence of the $D_o/t$ ratio on the response and stability of circular tubes that were subjected to symmetrical cyclic bending, Lee *et al.* [18] experimentally explored the effect of the $D_o/t$ ratio and curvature-rate on the response and stability of circular tubes subjected to cyclic bending, Chang *et al.* [19] studied the mean moment effect on circular, thin-walled tubes under cyclic bending, and Chang and Pan [20] discussed the buckling life estimation of circular tubes subjected to cyclic bending.

In practical industrial applications, tubes are under the hostile environment, so the material in the environment may corrode the tube surface and produce notches. Additionally, a tube in the working condition often involves some notches. The mechanical behavior and buckling failure of a notched tube differs from that of a tube with a smooth surface. In 2010, Lee *et al.* [21] studied the variation in ovalization of sharp-notched circular tubes subjected to cyclic bending. Lee [22] investigated the mechanical behavior and buckling failure of sharp-notched circular tubes under cyclic bending. Lee *et al.* [23] experimentally discussed the viscoplastic response and collapse of sharp-notched circular tubes subjected to cyclic bending. Later, Lee *et al.* [24] investigated the response of SUS304 stainless steel tubes subjected to pure bending creep and pure bending relaxation. However, all investigations were considered the circumferential sharp notch as shown in Fig. 1.

It is known that the tubes may be damaged by a sharp object during the delivery, installation or use. Once a cut is on a tube (Fig. 2), the response and failure of the sharp-cut circular tube under cyclic bending should be different from that of a smooth or circumferential sharp-notched

International Journal of Engineering Innovation & Research
Volume 5, Issue 1, ISSN: 2277 – 5668

circular tube under cyclic bending. Therefore, the response and failure of local sharp-cut circular tubes with different cut depths under cyclic bending was investigated in this paper.

Fig. 1. A picture of the circumferential sharp-notched circular tube.

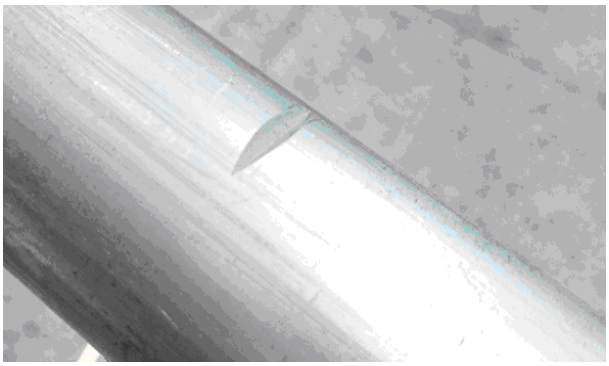

Fig. 2. A picture of the local sharp-cut circular tube.

## II. EXPERIMENT

### A. Bending Device

Fig. 3 is a schematic drawing of the bending device. It is designed as a four-point bending machine, capable of applying bending and reverse bending. The device consists of two rotating sprockets resting on two support beams. Heavy chains run around the sprockets and are connected to two hydraulic cylinders and load cells forming a closed loop. Each tube is tested and fitted with solid rod extension. The contact between the tube and the rollers is free to move along axial direction during bending. The load transfer to the test specimen is in the form of a couple formed by concentrated loads from two of the rollers. Once either the top or bottom cylinder is contracted, the sprockets are rotated, and pure bending of the test specimen is achieved. Reverse bending can be achieved by reversing the direction of the flow in the hydraulic circuit. Detailed description of the bending device can be found in Kyriakides and Shaw [1] and Pan *et al.* [14].

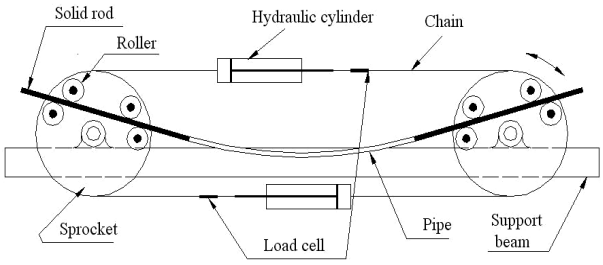


Fig. 3. Schematic drawing of the bending device.

### B. Curvature-Ovalization Measurement Apparatus (COMA)

The COMA, shown schematically in Fig. 4, is an instrument used to measure the tube curvature and ovalization of a tube cross-section. It is a lightweight instrument, which is mounted close to the tube mid-span. There are three inclinometers in the COMA. Two inclinometers are fixed on two holders, which are denoted side-inclinometers. These holders are fixed on the circular tube before the test begins. From the fixed distance between the two side-inclinometers and the angle change detected by the two side-inclinometers, the tube curvature can be derived. In addition, a magnetic detector in the middle part of the COMA is used to measure the change of the outside diameter. A more detailed description of the bending device and the COMA is given in Pan *et al.* [14].

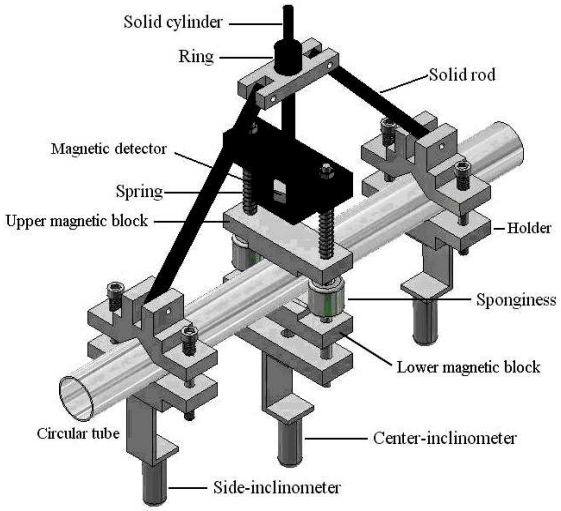


Fig. 4. Schematic drawing of the COMA.

### C. Material and Specimen

Circular tubes made of 6061-T6 aluminum alloy were adopted in this study. Table 1 shows the alloy's chemical composition in weight percentage. The ultimate stress is 258 MPa, the 0.2% strain offsetting yield stress is 166 MPa, and the percent elongation is 23%.

International Journal of Engineering Innovation & Research
Volume 5, Issue 1, ISSN: 2277 – 5668

Table 1: Chemical composition of 6061-T6 aluminum alloy (weight %).

| Chemical Composition | Al | Mg | Si | Ti | Fe |
|---|---|---|---|---|---|
| Proportion (%) | 98.096 | 0.937 | 0.535 | 0.012 | 0.139 |
| Chemical Composition | Mn | Zn | Cr | Ni | |
| Proportion (%) | 0.022 | 0.0983 | 0.022 | 0.005 | |

The raw, smooth 6061-T6 aluminum alloy circular tubes had an outside diameter $D_o$ of 35.0 mm and a wall thickness $t$ of 3.0 mm. The raw tubes were machined on the outside surface to obtain the desired shape and depth of the cut. Fig. 5 shows a schematic drawing of the sharp-cut circular tube, where the cut depth is denoted as $a$. In this study, five different cut depths were considered: 0.4, 0.8, 1.2, 1.6, and 2.0 mm. Fig. 6 shows a picture of the tested 6061-T6 aluminum alloy circular tubes with different cut depths.

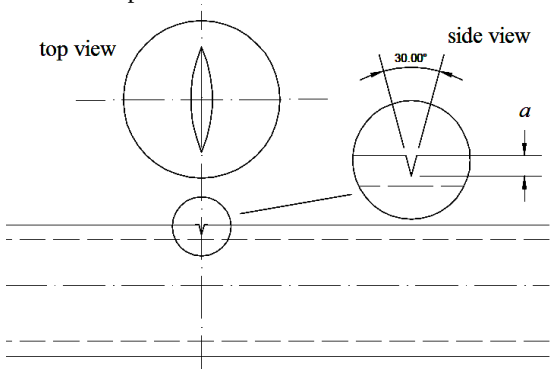


Fig. 5. Schematic drawing of a tube with a sharp-cut depth of $a$.

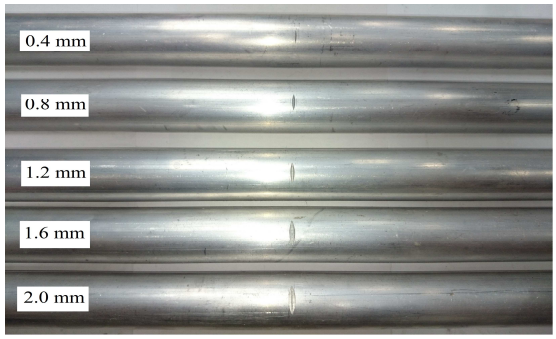


Fig. 6. Picture of the tested 6061-T6 aluminum alloy circular tubes with different cut depths.

### D. Test Procedures

The test involved a curvature-controlled cyclic bending. The controlled-curvature ranges were from ± 0.2 to ± 1.1 $m^{-1}$, and the curvature-rate of the cyclic bending test was 0.035 $m^{-1}s^{-1}$. The magnitude of the bending moment was measured by two load cells mounted to the bending device. The magnitude of the curvature and ovalization of the tube cross-section were controlled and measured by the COMA. In addition, the number of cycles required to produce failure was recorded.

## III. Finite Element Analysis

The Finite element software ANSYS was used to simulate the response of local sharp-cut circular tubes subjected to cyclic bending. The tubes' response was expressed in terms of the relationships between moment, curvature, and ovalization. The stress-strain relationship, the ANSYS mesh, boundary condition and loading condition are discussed in the following subsections

### A. Stress-Strain Relationship

A uniaxial stress-strain curve was constructed multilinearly in ANSYS according to the tested uniaxial stress-strain curve for 6061-T6 aluminum alloy in Fig. 7. Additionally, the kinematic hardening rule was used for cyclic loading.

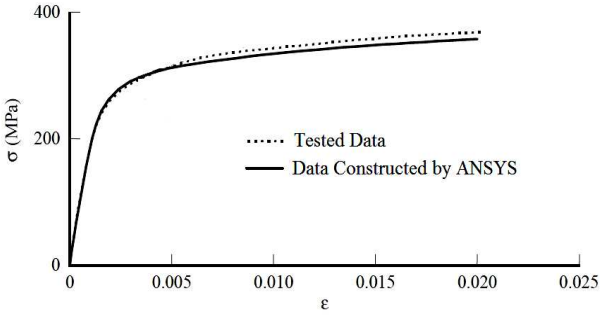


Fig. 7. Tested and ANSYS data of uniaxial stress-strain curves for 6061-T6 aluminum alloy.

### B. Mesh

Due to the three-dimensional geometry and elastoplastic deformation of the tube, the SOLID 186 element was used in the related analysis. This element is a tetrahedral element built in ANSYS and is suitable for analyzing plastic and large deformations. In particular, this element is adequate for analysis of shell components under bending. Due to the symmetry of the tube's left/right quarter, only half of the tube's model was constructed. Fig. 8 shows the mesh constructed by ANSYS for half tube.

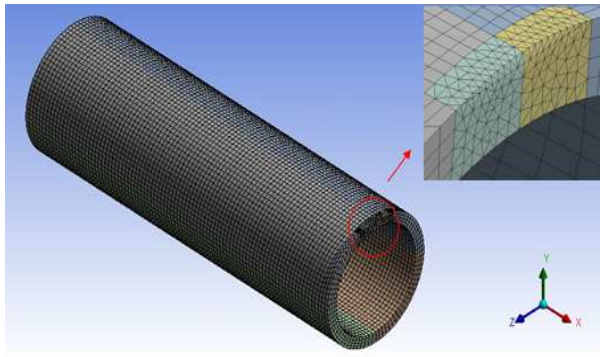

Fig. 8. Mesh constructed by ANSYS.

### C. Boundary Condition

Fig. 9 shows the restrictions on the symmetrical plane (central cross-section), constructed by ANSYS for a tube subjected to cyclic bending. Since the tubes were bent in

International Journal of Engineering Innovation & Research
Volume 5, Issue 1, ISSN: 2277 – 5668

the z-direction only, the frictionless roller support was fixed to the symmetrical plane and the displacement in the z-direction of this plane was set to zero.

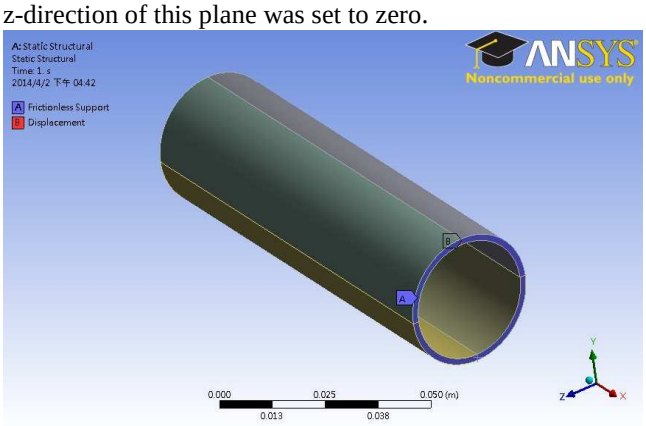


Fig. 9. Boundary condition constructed by ANSYS.

### D. *Loading Condition*

Fig. 10 shows the loading condition constructed by ANSYS on the basis of the tube bending device. As the figure shows, the remote displacement in the z-direction was unrestricted, i.e., the rotation was free to move in the z-direction. In addition, the bending moment was applied only in the z-direction and hence, the rotations in the x- and y-directions were set to zero.

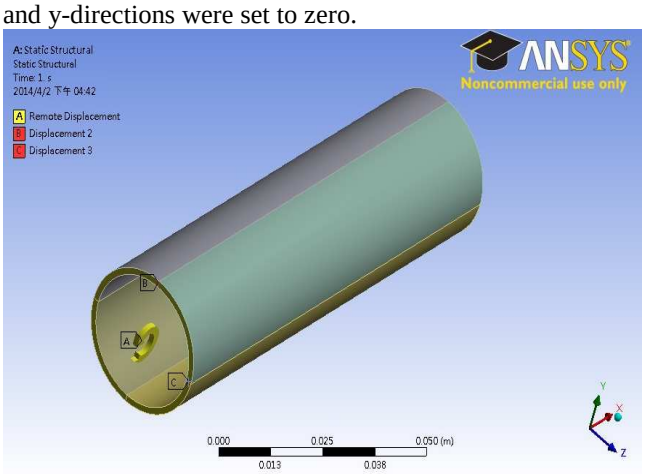


Fig. 10. Loading condition constructed by ANSYS.

The rotating angle $\theta$ in the z-direction (Fig. 11) was used as the input data (loading condition) for the tube under curvature-controlled cyclic bending. The relationship between $\theta$ and curvature $\kappa$ is

$$\kappa = 1 / \rho = 2\theta / L_o \quad (1)$$

where $L_o$ is the original tube length.

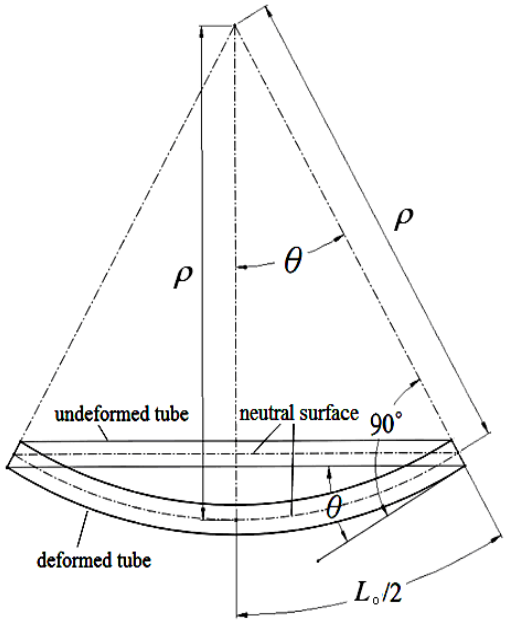


Fig. 11. Relationship between rotating angle $\theta$ and curvature $\kappa$ for a tube under pure bending.

## IV. Experimental and Theoretical Analysis

### A. *Moment, Curvature and Ovalization*

Fig. 12(a) shows a typical set of experimentally determined cyclic moment ($M$) - curvature ($\kappa$) curves for a local sharp-cut 6061-T6 aluminum alloy circular tube, with cut depth of $a$ = 0.4 mm, subjected to cyclic bending. The controlled minimum and maximum values of curvature were -0.4 $m^{-1}$ and +0.4 $m^{-1}$, respectively. It was observed that the $M$-$\kappa$ curve exhibited cyclic hardening and became gradually steady after a few bending cycles for symmetrical curvature-controlled cyclic bending. Fig. 12(b) shows the corresponding simulated $M$-$\kappa$ curve by ANSYS.

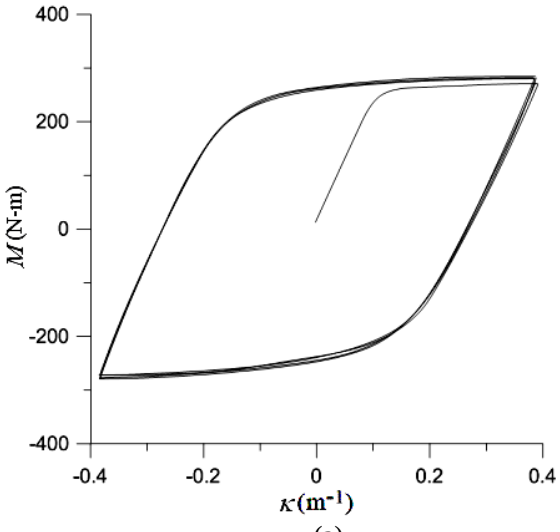


(a)

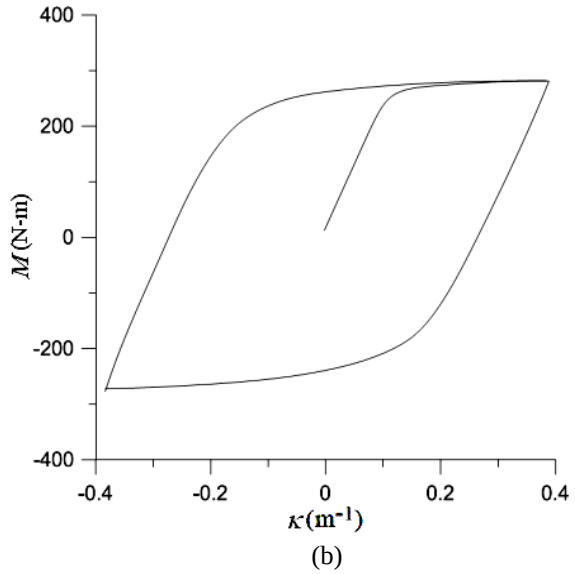


(b)

Fig. 12. (a) Experimental and (b) ANSYS simulated moment ($M$) - curvature ($\kappa$) curves for a local sharp-cut 6061-T6 aluminum alloy circular tube with $a$ = 0.4 mm under cyclic bending.

Fig. 13(a) show a typical set of experimentally determined cyclic ovalization ($\Delta D_o/D_o$) - curvature ($\kappa$) curve for a local sharp-cut 6061-T6 aluminum alloy circular tube, with cut depth of $a$ = 0.4 mm, subjected to cyclic bending. The ovalization is defined as $\Delta D_o/D_o$, where $D_o$ is the outside diameter and $\Delta D_o$ is the change in the outside diameter. The controlled minimum and maximum values of curvature were still -0.4 $m^{-1}$ and +0.4 $m^{-1}$, respectively. It was observed that the ovalization increased in a ratcheting manner with the number of bending cycles. Fig. 13(b) shows the corresponding simulated $\Delta D_o/D_o$-$\kappa$ curve by ANSYS. It can be seen that the ANSYS simulated results exhibit good correspondence to those obtained from the experiments.

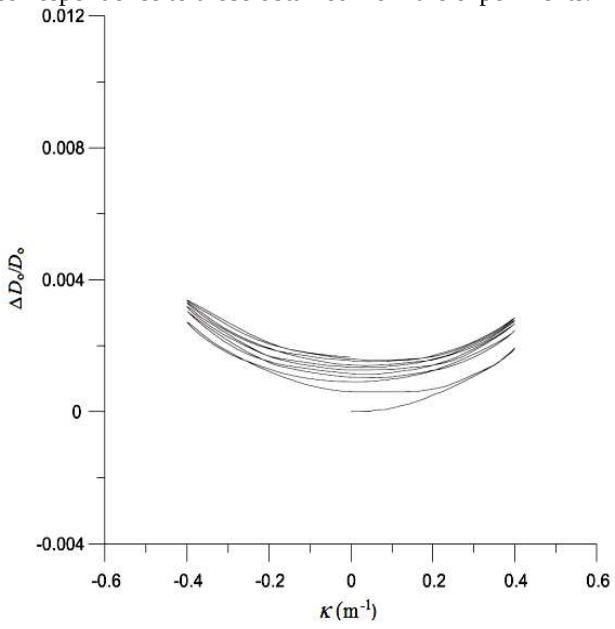


(a)

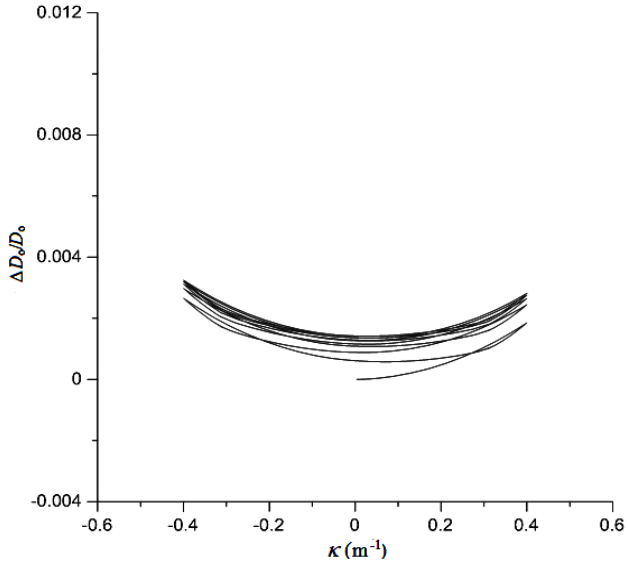


(b)

Fig. 13. (a) Experimental and (b) ANSYS simulated ovalization ($\Delta D_o/D_o$) - curvature ($\kappa$) curves for a local sharp-cut 6061-T6 aluminum alloy circular tube with $a$ = 0.4 mm under cyclic bending.

## B. *Fatigue Failure*

Fig. 14 shows a picture of the failure for local sharp-cut 6061-T6 aluminum alloy circular tubes with $a$ = 0.4, 0.8, 1.2, 1.6 and 2.0 mm under cyclic bending. The red circles denote the initiation of the crack. It was found that the crack initiated at the one or both sides of the cut. In addition, once the crack initiation was observed, the tube broke rapidly.


Fig. 14. A picture of the failure for local sharp-cut 6061-T6 aluminum alloy circular tubes with $a$ = 0.4, 0.8, 1.2, 1.6 and 2.0 mm under cyclic bending.

Table 2 shows the maximum and minimum stresses for local sharp-cut 6061-T6 aluminum alloy circular tubes subjected to cyclic bending. The magnitudes of stress were determined by ANSYS discussed in Sec. III. It was observed that for a given cut depth, a tube with a higher value of control curvature led to higher values of maximum and minimum stresses. In addition, for a given control curvature, a tube with a higher value of cut depth

led to higher values of maximum and minimum stresses. Due to the symmetrical curvature-controlled cyclic bending (the maximum control curvature equals to the minimum control curvature) and a local and small cut, the amounts of maximum and minimum stresses were almost the same for each loading case. Therefore, the mean stress effect did not consider in the failure analysis.

Table 2: Maximum and minimum stresses for local sharp-cut 6061-T6 aluminum alloy circular tubes under cyclic bending.

| Cut Depth (mm) | Control Curvature ($m^{-1}$) | Maximum stress (MPa) | Minimum stress (MPa) |
|---|---|---|---|
| 0.4 | ±1.01 | 184.34 | -184.14 |
| 0.4 | ±0.9 | 150.03 | -149.88 |
| 0.4 | ±0.7 | 131.98 | -131.66 |
| 0.4 | ±0.6 | 130.34 | -129.99. |
| 0.4 | ±0.5 | 128.83 | -128.27 |
| 0.8 | ±0.7 | 164.08 | -164.02 |
| 0.8 | ±0.6 | 159.24 | -159.03 |
| 0.8 | ±0.5 | 154.98 | -154.66 |
| 0.8 | ±0.4 | 151.96 | -151.62 |
| 0.8 | ±0.35 | 149.55 | -149.21 |
| 1.2 | ±0.5 | 189.46 | -189.40 |
| 1.2 | ±0.4 | 172.81 | -172.41 |
| 1.2 | ±0.35 | 169.70 | -169.15 |
| 1.2 | ±0.3 | 166.23 | -166.13 |
| 1.2 | ±0.25 | 161.33 | -161.12 |
| 1.6 | ±0.5 | 225.98 | -225.55 |
| 1.6 | ±0.4 | 215.51 | -215.35 |
| 1.6 | ±0.35 | 199.47 | -199.33 |
| 1.6 | ±0.3 | 196.05 | -195.88 |
| 1.6 | ±0.25 | 190.27 | -189.98 |
| 2.0 | ±0.45 | 241.37 | -241.22 |
| 2.0 | ±0.35 | 227.40 | -227.11 |
| 2.0 | ±0.3 | 222.58 | -222.32 |
| 2.0 | ±0.25 | 202.25 | -202.17 |
| 2.0 | ±0.2 | 188.01 | -187.65 |

Fig. 15 shows the experimental data of the stress amplitude ($\sigma_a$) versus the number of cycles required to produce failure ($2N_f$) in solid black circles for sharp-cut 6061-T6 aluminum alloy circular tubes with different cut depths subjected to cyclic bending on a log-log scale. Note that $\sigma_a$ = (maximum stress – minimum stress) / 2. It was observed that a tube with a higher value of control curvature or cut depth led to a lower $N_f$. In addition, the experimental $\sigma_a$-$N_f$ data were almost in a straight line. Therefore, a simple fatigue model was proposed to be

$$\sigma_a = \sigma_f'(2N_f)^b \quad (2)$$

or

$$\log \sigma_a = \log \sigma_f' + b \log 2N_f \quad (3)$$

where $\sigma_f'$ and $b$ are the fatigue strength coefficient and exponent, respectively. The straight line in Fig. 15 was determined by least-square fit. The magnitudes of $\sigma_f'$ and $b$ were determined to be 316.43 MPa and -0.12, respectively.

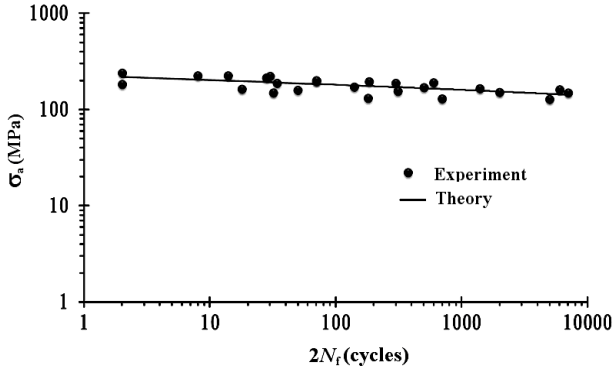


Fig. 15. Experimental and simulated stress amplitude ($\sigma_a$) versus the number of cycles required to produce failure ($2N_f$) for sharp-cut 6061-T6 aluminum alloy circular tubes with different cut depths under cyclic bending on a log-log scale.

## V. Conclusions

The failure of sharp-cut 6061-T6 aluminum alloy circular tubes with different cut depths subjected to cyclic bending was investigated in this study. On the basis of the experimental and theoretical results, the following conclusions can be drawn:

(1) The $M$-$\kappa$ curves of sharp-cut 6061-T6 aluminum alloy circular tubes exhibited cyclic hardening and became gradually steady after a few bending cycles for symmetrical curvature-controlled cyclic bending.

(2) The $\Delta D_o/D_o$-$\kappa$ curves of sharp-cut 6061-T6 aluminum alloy circular tubes showed that the ovalization of the tube cross-section increased in a ratcheting manner with the number of bending cycles.

(3) Using adequate stress-strain relationships, mesh, boundary conditions and loading conditions, the finite element software ANSYS was used for simulating the behavior of sharp-cut circular tubes subjected to cyclic bending; this behavior included the $M$-$\kappa$ and $\Delta D_o/D_o$-$\kappa$ relationships. The simulated results exhibited close correspondence to those obtained from experiments.

(4) According to the $\sigma_a$-$2N_f$ relationship for sharp-cut 6061-T6 aluminum alloy circular tubes with different cut depths under cyclic bending. A simple fatigue model (Eq. (2)) was proposed and parameters $\sigma_f'$ and $b$ were determined to be 316.43 MPa and -0.12, respectively. It was found that the simulation was in good agreement with the experimental result as shown in Fig. 15.

## VI. Acknowledgment

The work presented was carried out with the support of the National Science Council under grant MOST 104-2221-E-006-111. Its support is gratefully acknowledged.

## REFERENCES

[1] P.-K. Shaw, and S. Kyriakides, "Inelastic analysis of thin-walled tubes under cyclic bending," *Int. J. Solids Struct.*, vol. 21, no. 11, 1985, pp. 1073-1110.

[2] S. Kyriakides, and P.-K. Shaw, "Inelastic buckling of tubes under cyclic loads," *J. Pres. Ves. Tech.*, vol. 109, no. 2, 1987, pp. 169-178.

[3] E. Corona, and S. Kyriakides, "On the collapse of inelastic tubes under combined bending and pressure," *Int. J. Solid Struct.*, vol. 120, no. 12, 1988, pp. 1232-1239.

[4] E. Corona, and S. Kyriakides, "An experimental investigation of the degradation and buckling of circular tubes under cyclic bending and external pressure," *Thin-Walled Struct.*, vol. 12, no. 3, 1991, pp. 229-263.

[5] E. Corona, and S. Vaze, "Buckling of elastic-plastic square tubes under bending," *Int. J. Mech. Sci.*, vol. 38, no. 7, 1996, pp. 753-775.

[6] S. Vaze, and E. Corona, "Degradation and collapse of square tubes under cyclic bending," *Thin-Walled Struct.*, vol. 31, no. 4, 1998, pp. 325-341.

[7] E. Corona, and S. Kyriakides, "Asymmetric collapse modes of pipes under combined bending and pressure," *Int. J. Solids Struct.*, vol. 24, no. 5, 2000, pp. 505-535.

[8] E. Corona, L.-H. Lee, and S. Kyriakides, "Yield anisotropic effects on buckling of circular tubes under bending," *Int. J. Solids Struct.*, vol. 43, no. 22, 2006, pp. 7099-7118.

[9] S. Kyriakides, A. Ok, and E. Corona, "Localization and propagation of curvature under pure bending in steel tubes with Lüders bands," *Int. J. Solids Struct.*, vol. 45, no. 10, 2008, pp. 3074-3087.

[10] A. Limam, L.-H. Lee, E. Corana, and S. Kyriakides, "Inelastic wrinkling and collapse of tubes under combined bending and internal pressure," *Int. J. Mech. Sci.*, vol. 52, no. 5, 2010, pp. 37-47.

[11] J. F. Hallai, and S. Kyriakides, "On the effect of Lüders bands on the bending of steel tubes," *Int. J. Solids Struct.*, vol. 48, no. 24, 2011, pp. 3275-3284.

[12] A. Limam, L.-H. Lee, and S. Kyriakides, "On the collapse of dented tubes under combined bending and internal pressure," *Int. J. Solids Struct.*, vol. 55, no. 1, 2012, pp. 1-12.

[13] N. J. Bechle, and S. Kyriakides, "Localization of NiTi tubes under bending," *Int. J. Solids Struct.*, vol. 51, no. 5, 2014, pp. 967-980.

[14] W.-F. Pan, T.-R. Wang, and C.-M. Hsu, "A curvature-ovalization measurement apparatus for circular tubes under cyclic bending," *Exp. Mech.*, vol. 38, no. 2, 1998, pp. 99-102.

[15] W.-F. Pan, and C.-H. Fan, "An experimental study on the effect of curvature-rate at preloading stage on subsequent creep or relaxation of thin-walled tubes under pure bending," *JSME Int. J., Ser. A*, vol. 41, no. 4, 1998, pp. 525 -531.

[16] W.-F. Pan, and Y.-S. Her, "Viscoplastic collapse of thin-walled tubes under cyclic bending," *J. Eng. Mat. Tech.*, vol. 120, no. 4, 1998, pp. 287-290.

[17] K.-L. Lee, W.-F. Pan, and J.-N. Kuo, "The influence of the diameter-to-thickness ratio on the stability of circular tubes under cyclic bending," *Int. J. Solids Struct.*, vol. 38, no. 14, 2001, pp. 2401-2413.

[18] K.-L. Lee, W.-F. Pan, and C.-M. Hsu, "Experimental and theoretical evaluations of the effect between diameter-to-thickness ratio and curvature-rate on the stability of circular tubes under cyclic bending," *JSME Int. J., Ser. A*, vol. 47, no. 2, 2004, pp. 212-222.

[19] K.-H. Chang, W.-F. Pan, and K.-L. Lee, "Mean moment effect on circular thin-walled tubes under cyclic bending," *Struct. Eng. Mech.*, vol. 28, no. 5, 2008, pp. 495-514.

[20] K.-H. Chang, and W.-F. Pan, "Buckling life estimation of ircular Tubes under Cyclic Bending," *Int. J. Solids Struct.*, vol. 46, no. 2, 2009, pp. 254-270.

[21] K.-L. Lee, C.-Y. Hung, and W.-F. Pan, "Variation of ovalization for sharp-notched circular tubes under cyclic bending," *J. Mech.*, vol. 26, no. 3, 2010, pp. 403-411.

[22] K.-L. Lee, "Mechanical behavior and buckling failure of sharp-notched circular tubes under cyclic bending," *Struct. Eng. Mech.*, vol. 34, no. 3, 2010, pp. 367-376.

[23] K.-L. Lee, C.-M. Hsu, and W.-F. Pan, "Viscoplastic collapse of sharp-notched circular tubes under cyclic bending," *Acta Mech. Solida Sinica*, vol. 26, no. 6, 2013, pp. 629- 641.

[24] K.-L. Lee, C.-M. Hsu, and W.-F. Pan, "Response of sharp-notched circular tubes under bending creep and relaxation," *Mech. Eng. J.*, vol. 1, no. 2, 2014, pp. 1-14.

## AUTHORS' PROFILE

**Kuo-Long Lee** received the Ph.D. degree in Dept. of Engineering Science from National Cheng Kung University in Taiwan in 2000. Currently working as Prof. in Dept. of Innovative Design and Entrepreneurship from Far East University in Taiwan.

**Li-Yang Chen** received the B.S. degree in Dept. of Engineering Science from National Cheng Kung University in Taiwan in 2015. Currently registering as graduate student in Dept. of Engineering Science from National Cheng Kung University in Taiwan.

**Wen-Fung Pan** received the Ph.D. degree in Dept. of Civil and Environmental Engineering from University of Iowa in USA in 1989. Currently working as Prof. in Dept. of Engineering Science from National Cheng Kung University in Taiwan.